THE STRUCTURE OF EVAPORATING AND COMBUSTING SPRAYS: MEASUREMENTS AND PREDICTIONS

Semi-Annual Status Report

For the Period

September 1, 1981 to February 28, 1982

by

J-S. Shuen, A. S. P. Solomon and G. M. Faeth
Department of Mechanical Engineering
The Pennsylvania State University
University Park, Pennsylvania 16802

Prepared for

National Aeronautics and Space Administration
Grant No. NAG 3-190
NASA Lewis Research Center
R. Tacina, NASA Scientific Officer

March 1982

Semi-Annual Status Report on The Structure of Evaporating and Combusting Sprays: Measurements and Predictions

SUMMARY

This report covers the first semi-annual period of an investigation of the properties of noncombusting and combusting sprays. Activities during this period were limited to noncombusting sprays. An apparatus was constructed to provide measurements in open sprays with no zones of recirculation, in order to provide well-defined conditions for use in evaluating spray models. The measurements in noncombusting sprays include: mean and fluctuating gas velocities, mean and fluctuating drop velocities, drop sizes, mean liquid fluxes, mean temperatures and mean compositions. Thus far, measurements have been completed in a gas jet, in order to test experimental methods, and are currently in progress for nonevaporating sprays.

Models of the process are also being examined including: (1) a locally homogeneous flow (LHF) model where interphase transport rates are assumed to be infinitely fast; (2) a separated flow (SF) model which allows for finite interphase transport rates but neglects effects of turbulent fluctuations on drop motion; and (3) a stochastic SF model which considers effects of turbulent fluctuations on drop motion. In this report, the models are evaluated using existing data on particle-laden jets. The LHF model generally overestimated rates of particle dispersion while the SF model underestimated dispersion rates. In contrast, the stochastic SF flow yielded satisfactory predictions except at high particle mass loadings where effects of turbulence modulation may have caused the model to overestimate turbulence levels--and thus dispersion rates. This evaluation is tentative, however, due to uncertainties in the specification of initial conditions for the existing data base.

Current work is addressing both existing and present new measurements in nonevaporating sprays. These results should indicate the importance of drop collisions and shattering, as well as effects of turbulence modulation.

TABLE OF CONTENTS

LIST OF FIGURES

LIST OF TABLES

NOMENCLATURE

Symbol	Description
a	acceleration of gravity
C	particle concentration
C_D	drag coefficient
C_i	parameters in turbulence model
C_p	specific heat
d	injector diameter
d_p	drop diameter
D	binary diffusivity
$e_{b\lambda}$	monochromatic blackbody emissive power
f	mixture fraction
g	square of mixture fraction fluctuations
G	particle mass flux
h	heat transfer coefficient
h_s, h_p	enthalpy
H	total enthalpy
I_λ	monochromatic radiation intensity
K_λ	monochromatic absorption coefficient
k	turbulence kinetic energy
L_e	dissipation length scale
m	drop mass
$\dot{m}$	drop evaporation rate
$\dot{m}_o$	injector flow rate
$\dot{M}_o$	injector thrust
$\dot{n}_i$	number of drops per unit time in class i

Symbol	Description
$P(f)$	probability density function of f
Pr	Prandtl number
Re	Reynolds number
r	radial distance
s	distance along beam path
Sc	Schmidt number
S_ϕ	source term
$S_{d\phi}$	droplet source term
t	time
t_e	eddy lifetime
t_t	drop transit time
T	gas temperature
T_p	drop temperature
u	axial velocity
$\vec{u}_p$	drop velocity vector
v	radial velocity
v^o	Favre radial velocity
x	axial distance
$\vec{x}_p$	drop position vector
$\bar{y}^2$	variance of radial particle position
Y_i	mass fraction of species i
α	weighting factor, Eq. (6)
ε	rate of dissipation of turbulence kinetic energy
λ	thermal conductivity
μ_t	turbulent viscosity
ρ	density

Symbol	Description
τ	particle relaxation time
σ_i	turbulent Prandtl/Schmidt number
ϕ	generic property

Subscripts

c	centerline quantity
f	liquid
g	vapor
p	drop property
s	drop surface
0	injector exit condition
∞	ambient condition

Superscripts

$( )'$	fluctuating quantity
$(\bar{})$	time mean value

1. Introduction

The potential value of rational design procedures for liquid-fueled combustors has motivated continuous efforts to develop reliable models of spray evaporation and combustion processes. The goal is to reduce the time and cost of cut and try methods of development by providing a better understanding of fundamental spray processes and methods for estimating the effect of specific design changes. While there has been significant progress in the development of spray models, no existing model has demonstrated a capability for reliable predictions (or even correlation) of spray behavior, largely due to the unavailability of appropriate measurements for model evaluation. The objective of this investigation is to complete measurements in evaporating and combusting sprays in order to close this gap in the existing information.

Current activity concerning spray modeling is quite high, as evidenced by the recent development of relatively sophisticated models of sprays in industry [1-5]. Reviews of spray modeling [6-11] find 10-20 papers per year reporting new spray models at present, when contributions from government and universities are considered. While the basic elements of spray models are in hand, much work must still be done to improve the treatment of interphase transport, turbulence, chemical reaction and radiation processes in sprays [6-11].

Properly establishing models by comparing predictions with experiments has substantially lagged model development. The major problem is that measurements in sprays, particularly combusting sprays, present formidable experimental difficulties. A second problem is that experimenters have not adequately recognized the need for specifying the properties of the injector. Spray models are so dependent on injected drop sizes and velocities that measurements without this information are of little value for testing spray models.

The objective of this investigation is to complete new measurements in order to improve the data base available for model development. A main feature of the experiments is that a steady axisymmetric spray, with no zones of recirculation, is considered. Such conditions minimize experimental difficulties, reduce uncertainties in modeling the turbulent flow, and simplify requirements for obtaining accurate numerical solutions of the transport equations. Analysis of the experimental results is also being undertaken using models whose development was initiated during past NASA-sponsored research in this laboratory.

The investigation is planned for a two-year period, with noncombusting sprays examined during the first year and combusting sprays during the second year. This report covers the first semi-annual period of the investigation where attention was primarily devoted to analysis of particle-laden flows and measurements in nonevaporating sprays. This report considers experimental and theoretical methods used during the investigation, along with a description of the results obtained to date. A paper describing a portion of these results was also prepared during this report period, cf. Ref. 15.

---

*Numbers in brackets denote references.

2. Experimental Methods

2.1 Test Apparatus

A sketch of the spray apparatus appears in Fig. 1. The present noncombusting flows all have densities greater than air; therefore, the injector is directed downward in still air, in order to avoid recirculation. The measurements enploy optical instrumentation which must be mounted on a rigid base. Therefore, probing the flow is accomplished by traversing the injector in three dimensions.

The flow is protected from room disturbances using a screened enclosure (1 m square by 2.5 m high). Major traversing, to obtain radial profiles of flow quantities, involves moving the entire cage assembly. This keeps the flow nearly concentric with the vertical axis of the cage, which minimizes disturbance of the axisymmetric flow due to off-center screen positions.

The inlet to the exhaust system is screened and is located 1 m below the plane of instrumentation. Testing has shown that operation of the exhaust system has a negligible effect on flow properties at the measuring plane.

A Spraying Systems Co. air atomizing injector (model 1/4J2050 fluid nozzle and 67147 air nozzle with outlet diameter of 1.19 mm) is being used for the spray tests--similar to earlier work [12,13]. An attempt was made to employ a flashing injector developed earlier [16]; however, this arrangement proved to be unsatisfactory due to complications of external expansion from a choked injector for conditions yielding desired atomization properties.

The flow system of the injector is illustrated in Fig. 2. Filtered dry air is supplied from a storage tank. The flow rate of air is controlled with a pressure regulator and metered with a critical-flow orifice to ensure long-term stable operation.

The liquid is stored in a tank under pressure, however, the tank is not agitated and pressure levels are moderate (0.3-0.8 kPa). Therefore, the dissolved air content of the liquid is negligible. The flow rate of liquid is controlled with a valve and metered with a rotameter. In order to maintain repeatable flow and atomization conditions the entire test cell is heated above normal ambient temperatures - to 27 $\pm 1^{\circ}$C.

The test liquid for measurements with nonevaporating sprays is vacuum pump oil. This material has reasonable pumping characteristics and very low volatility. Freon 11 will be used for tests of evaporating noncombusting sprays, since it has sufficient volatility to evaporate rapidly in room temperature air while posing no explosion hazards. Freon 11 was also used in previous experiments with sprays in this laboratory [12].

2.2 Instrumentation

Table 1 is a summary of the measurements that are being undertaken in noncombusting sprays and the techniques employed for each measurement.

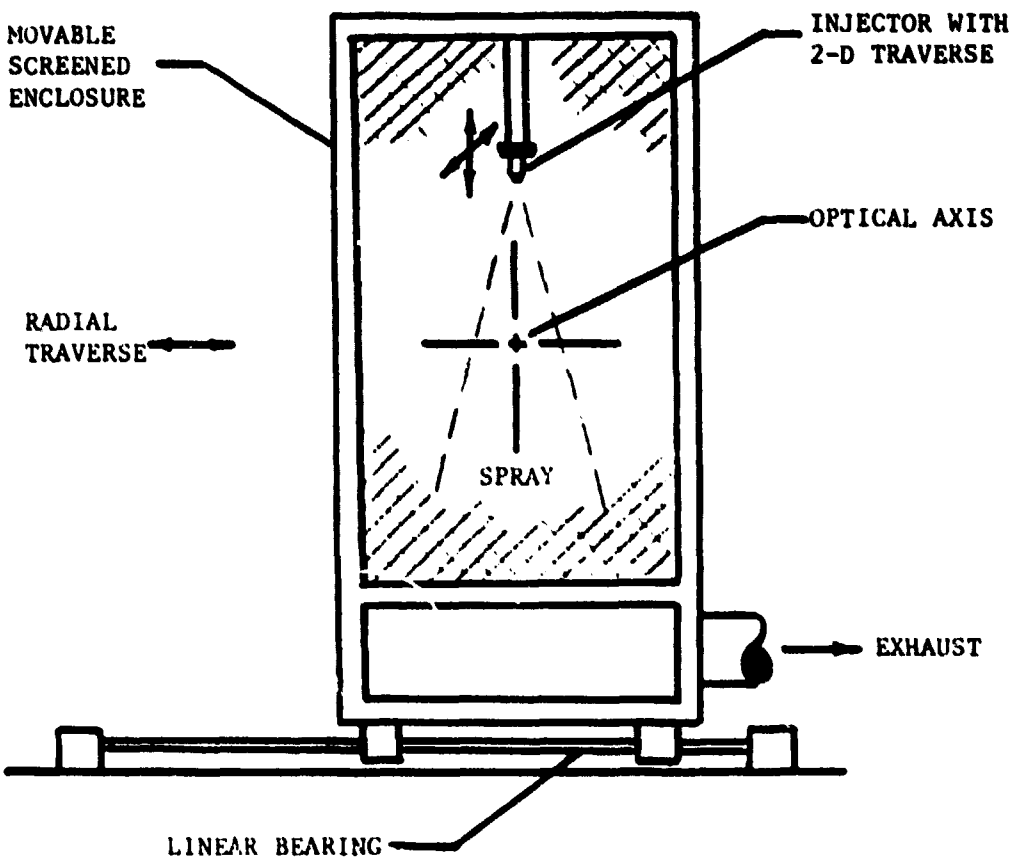

Fig. 1 Sketch of the experimental apparatus.

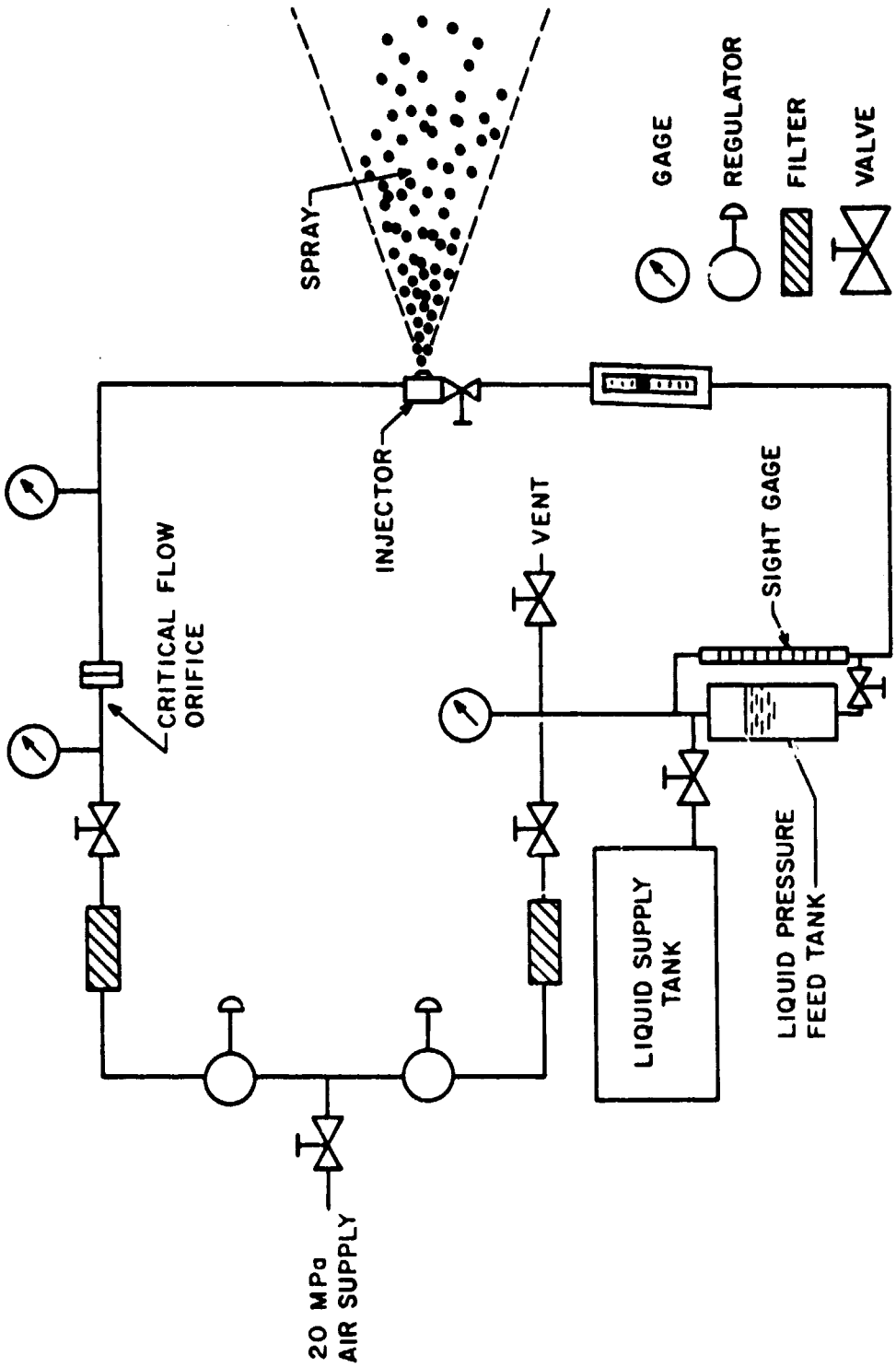

Fig. 2 Sketch of the injector flow system.

Table 1. Summary of Instrumentation for Noncombusting Sprays

Measurement	Technique	Equipment
Mean and fluctuating gas velocities[a]	Dual-beam, forward scatter laser Doppler anemometer, frequency shifted with tracker and burst counter data processing.	Spectra Physics Model 125A (50 mW) He Ne laser, rest TSI Inc.
Drop size and velocity	Streak photographs.	Photosonic Model 16b camera with rotating prism removed. Hg arc back-lighting.
Drop size and velocity	Laser-Doppler anemometer visibility technique.	TSI Inc. equipment.
Drop size distributions[a]	Fraunhofer diffraction.	Malvern Model 2200 Particle Sizer.
Liquid flux-nonevaporating conditions	Isokinetic sampling and inertial separation.	In-house design.
Liquid flux--evaporating conditions[a]	Slide impaction.	In-house design.
Mean temperature--evaporating conditions[a]	Fine-wire thermocouple shielded from drop impacts.	In-house design, 76 micron diameter wires.
Mean composition of major species--evaporating spray[a]	Isokinetic sampling and analysis with gas chromatograph.	Perkin-Elmer Model 880 chromatograph with hot-wire detector.

[a]Method used in past work in this laboratory, cf. Refs. 8-16 for further details.

A laser Doppler anemometer is used to measure mean and fluctuating gas velocities. Several beam orientations provide measurements of various velocity components as well as the Reynolds stress. In order to avoid problems of fringe bias and reverse flows, the laser beams are frequency shifted. Concentration biasing and effects of drops are avoided by employing high concentrations of seeding particles--following past methods [12,13].

Accurate measurement of initial conditions requires good spatial resolution in the dense portion of the spray. Imaging techniques are most effective in this region [17]. Therefore, drop properties are determined by high-magnification, direct-lighted streak photographs near the injector. This method is tedious, however, it is the most reliable technique available for providing initial conditions relatively near the injector.

A second method used for drop size and velocity measurements involves the LDA--visibility technique [18]. This technique is relatively independent of the refractive indices of the disperse and continuous phases and can be used in noncombusting sprays. The technique provides a simultaneous indication of drop size and velocity far more conveniently than the imaging method--in dilute sprays. This equipment is currently being acquired--funded by University resources--and the system is not yet operational. However, we hope to complete a portion of the noncombusting spray measurements during the next report period with this instrument.

Drop sizes are also measured with a Malvern particle size analyzer, which operates on the principle of Fraunhofer diffraction of laser light scattered by drops. This instrument only provides a line-of-sight measurement and is largely used to monitor injector performance.

Liquid fluxes are measured by isokinetic sampling and by impaction. These techniques are well-established in the literature and provide a check of the newer optical methods. The sampling probe has a 2 mm ID sampling port, followed by a nitrogen-flushed diverging section to prevent drop impaction on the internal surfaces of the probe. The drops are collected in an internal spill-over probe, backed up by a filter to collect small-diameter drops. Isokinetic sampling conditions are determined by fixing the probe just below the LDA measuring volume and matching disturbed and undisturbed gas velocities.

It is difficult to obtain accurate mean temperature measurements in sprays due to effects of drop impaction. We have developed a shielded temperature probe which circumvents most of these problems [12,13]. This involves a 50 μm diameter Pt/Pt 10% Rh butt-welded thermocouple located along the centerline of a 1.6 mm OD semi-circular shield. The shield is positioned upstream of the probe so that all but the smallest drops (diameter less than 10 μm generally) impinge on it. Therefore, the thermocouple primarily senses gas temperatures. The probe has been checked in gas flames and found to yield temperatures within 10 K of unshielded temperatures, indicating that effects of flow deflection and increased heat losses are small for current experimental conditions.

The mean composition of injected fluid in the evaporating sprays is determined by isokinetic sampling, at the mean gas velocity, and analysis with a gas chromatograph. The probe is heated to prevent blockage with liquid. This tec ique provides a direct measurement of the local mixture fraction of the flow. The system used is identical to Shearer et al. [12].

3. Theory

3.1 General Description

Present measurements as well as results in the literature are being used to evaluate spray models. Two models are considered: (1) a locally homogeneous flow (LHF) model, where both phases are assumed to have the same velocity and temperature and are in thermodynamic equilibrium at each point in the flow;* and (2) a separated flow (SF) model where finite interphase transport rates are considered, so that each phase generally has a different velocity and temperature throughout the flow.

Both models employ the widely adopted procedures of k-ε-g turbulence models for the gas phase [12-15,19,20], since this approach has been thoroughly calibrated during earlier work in this laboratory [12-15]. Major assumptions for the gas phase are: exchange coefficients of all species and heat are the same, buoyancy only affects the mean flow, and kinetic energy and heat losses are negligible. Effects of buoyancy and radiation heat losses are generally small in practical sprays; therefore, treating these phenomena as perturbations is justified. Neglecting kinetic energy limits the model to low Mach number flows, which is appropriate for the test conditions to be examined, as well as most practical combustion chambers. The assumption of equal exchange coefficients is widely recognized as being appropriate for high Reynolds number turbulent flows typical of spray processes.

Two versions of the separated flow model have been developed. One version considers mean particle trajectories similar to past models while the second version treats effects of turbulent fluctuations using stochastic methods.

In order to ensure adequate numerical closure with reasonable computation costs, the model is limited to boundary-layer flows with no recirculation. The present test flows are axisymmetric with no swirl; therefore, the analysis is posed accordingly. An advantage of these conditions is that they correspond to cases where k-ε-g models were developed and have high reliability.

3.2 Locally Homogeneous Flow Model

The governing equations, under the LHF approximation, can be written as follows:

---

*This approximation is only valid for infinite interphase transport rates--implying a flow with infinitely small particles or drops.

$$\frac{\partial}{\partial x}(\bar{\bar{\rho}}\bar{\bar{u}}\bar{\phi}) + \frac{1}{r}\frac{\partial}{\partial r}(r\bar{\bar{\rho}}\bar{\bar{v}}^{o}\bar{\phi}) = \frac{1}{r}\frac{\partial}{\partial r}\left(r\frac{\mu_t}{\sigma_\phi}\frac{\partial \phi}{\partial r}\right) + S_\phi \tag{1}$$

where

$$\bar{\bar{\rho}}\bar{\bar{v}}^{o} = \bar{\bar{\rho}}\bar{\bar{v}} + \overline{\rho' v'} \tag{2}$$

The parameters ϕ and S_ϕ appearing in Eqs. (1) and (2) are summarized in Table 2, along with the appropriate empirical constants. The empirical constants were established for noncombusting single-phase flows and are not changed when sprays are considered [12,13,20]. The turbulent viscosity is calculated from the turbulent kinetic energy and rate of dissipation as follows:

$$\mu_t = C_\mu \bar{\rho} k^2/\epsilon \tag{3}$$

With equal exchange coefficients and moderate radiative heat losses, which is normally the case even for combusting sprays, instantaneous properties are only a function of mixture fraction (essentially the state resulting from adiabatic equilibration of f kg of injector fluid and (1-f)fg of ambient fluid). This allows determination of all properties, temperature, composition and density, as a function of mixture fraction--once and for all. Properties in the flow are then found from the probability density function for mixture fraction, P(f) as follows [20]

$$\bar{\phi} = \int_0^1 \phi(f)P(f)\,df \tag{4}$$

where $\phi(f)$ is known from the state relationship. A functional form must be assumed for P(f). A clipped Gaussian function, similar to Lockwood and Naguib [20], is being used for P(f), although the specific form used has little effect on predictions. P(f) depends on two parameters which can be found from the local values of f and g as described by Lockwood and Naguib [20].

The computation of the state relationships, $\phi(f)$ involves only conventional adiabatic mixing (noncombusting spray) or adiabatic flame (combusting spray) calculations. The methods used for these computations are described elsewhere [11-14,21,22]. In the case of combusting sprays, the state relationship calculations employ CEC-72 [23], which allows for variable specific heats and dissociation in high-temperature gases.

A typical state relationship is illustrated in Fig. 3. The case shown is for a Freon 11 spray injected into air at atmospheric pressure, using an air-atomizing injector [12]. Evaporation of Freon 11 in the atomizing air yields a mixture of air and Freon-11 liquid and vapor

Table 2. Source Terms in Eq. (1)

ϕ	S_ϕ
1	0
$\bar{u}$	$\pm$ a $(\rho_\infty - \bar{\rho})$
k	$\mu_t \left(\frac{\partial \bar{u}}{\partial r}\right)^2 - \bar{\rho}\varepsilon$
$\bar{f}$	0
g	$C_{g_1} \mu_t \left(\frac{\partial \bar{f}}{\partial r}\right)^2 - C_{g_2} \bar{\rho} \frac{\varepsilon g}{k}$

Notes:

1. Positive sign is used in $S_{\bar{u}}$ for vertical upward flow.
2. Turbulence model constants are assigned the following values: $C_\mu = 0.09$, $C_{\varepsilon_1} = 1.44$, $C_{g_1} = 2.8$, $\sigma_k = 1.0$, $\sigma_\varepsilon = 1.3$, $\sigma_{\bar{f}} = 0.7$, $\sigma_g = 0.7$ and $C_{\varepsilon_2} = C_{g_2} = 1.84$.

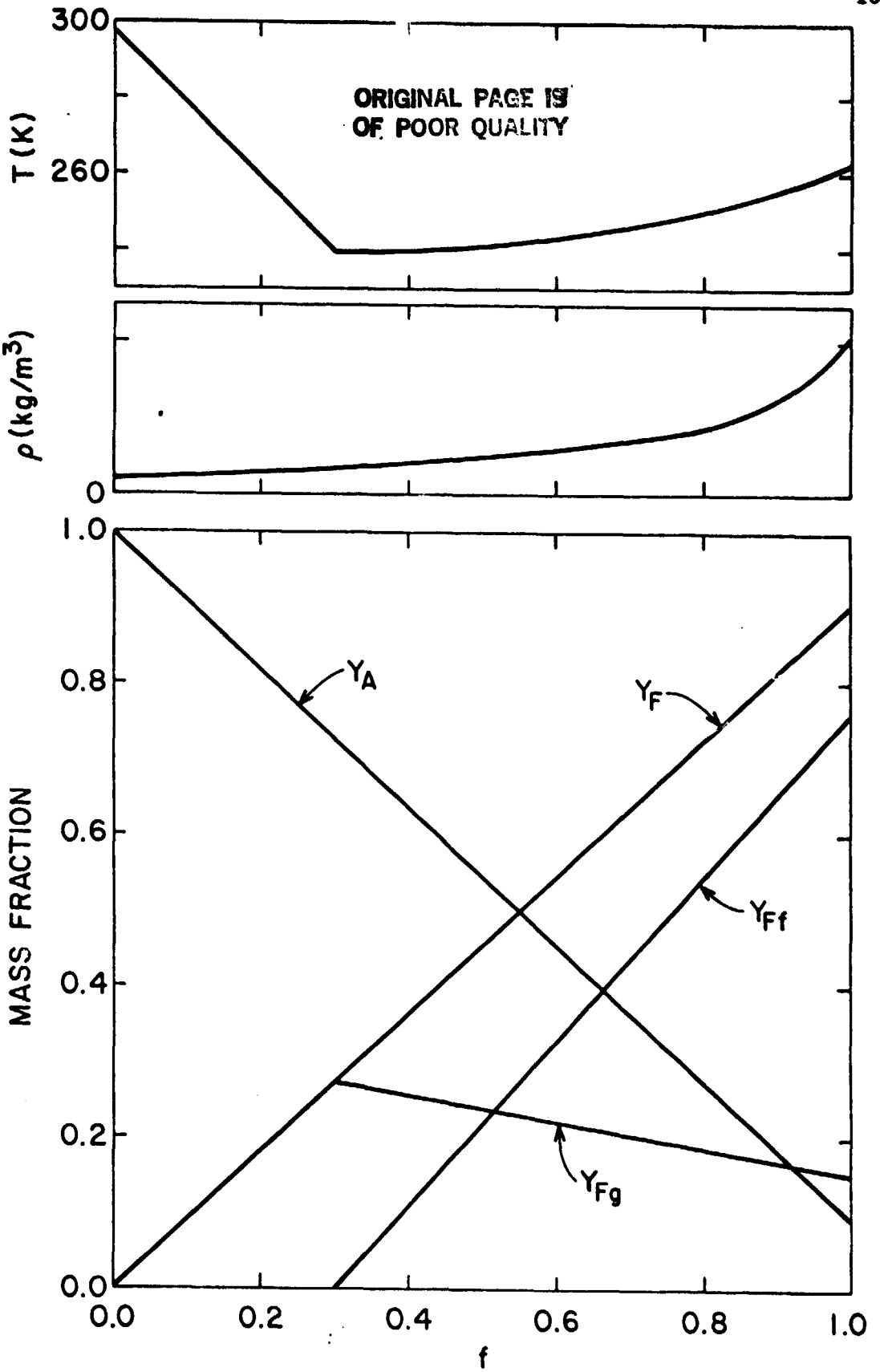

Fig. 3 Scalar properties as a function of mixture fraction for a Freon 11 spray evaporating in air at atmospheric pressure. From Shearer et al. [12].

leaving the injector at a temperature somewhat below their initial 300 K temperature (at f = 1). The surroundings are pure air at 300 K (at f = 0). As fluid mixes with the injector flow, the concentration of liquid and the temperature decrease until the point is reached where all the liquid has evaporated ($f \tilde{} 0.3$), which also corresponds to the maximum Freon 11 vapor concentration. At lower mixture fractions, the temperature increases and the Freon 11 vapor concentration decreases toward the ambient values. The presence of liquid in portions of the mixture fraction range causes a very nonlinear density variation. Similar state relationships for combusting flows at moderate and high pressures are presented elsewhere [11,13,14].

Initial conditions for the calculations are prescribed at the injector exit similar to past work [11-14]. In the absence of other information, all properties are assumed to be constant at the injector exit, aside from a shear layer having a thickness equal to 1 percent of the injector radius at the passage wall. The constant property portion of the flow is specified as follows:

$$x = 0,\ r < 0.99d/2;\ \bar{u}_o = \dot{M}_o/\dot{m}_o,\ \bar{f}_o = 1,\ k_o = (0.02\bar{u}_o)^2$$

$$g_o = 0\ ,\quad \varepsilon_o = 2.84 \times 10^{-5}\ \bar{u}_o^{\,3}/d \tag{5}$$

The initial variation of properties in the shear layer is assumed to be linear. Equation (5) provides the inner boundary condition until the shear layer reaches the spray axis, after which all gradients at the axis are zero. The ambient values of $\bar{u}$, $\bar{f}$, k, ε and g are all zero for the flows to be considered here. The calculations are performed using a modified version of GENMIX [24].

The main advantage of the LHF model is that there are only a few empirical constants, which are specified by earlier measurements, and only routine equilibrium computations and simplified injector quantities are required for computations. In view of its ease of use, the model has demonstrated reasonably good capabilities for computing spray properties [12-14]. The main defect is that the rate of flow development is overestimated in the two-phase region. Potential users of spray models are likely to begin with a version of this type, therefore, it is desirable to evaluate its performance.

3.3 Separated Flow Model

The separated flow model adopts the main features of the LHF model, but only for the gas phase. The liquid phase is treated by solving the Lagrangian equations of motion of the drops and then computing the source terms in the governing equations for the gas phase, resulting from interphase transport processes. This general procedure corresponds to the particle tracking or particle-source-in-cell methods used in most recent two-phase models and is often called a discrete droplet model (DDM) [11].

Drop Model. The main assumptions of the drop trajectory calculations are as follows: dilute spray with drop transport parameters equivalent to a single drop in an infinite environment; ambient conditions given by mean flow properties; negligible effect of turbulent fluctuations on drop transport rates; empirical treatment of drag and convection effects; quasisteady gas phase; negligible drop shattering and collisions; liquid surface in thermodynamic equilibrium; and negligible radiation, Dufour and Soret effects. These assumptions are common in spray models--their justification is discussed elsewhere [7,11].

The assumption of unity Lewis number is not made, since liquid fuels are often modeled poorly in this manner due to their large molecular weights. Average gas-phase properties for drop transport calculations are found at a reference state defined by

$$\phi_{avg} = \alpha \phi_{pg} + (1 - \alpha) \bar{\phi}_{\infty} \tag{6}$$

where ϕ is a generic property representing temperature and species mass fractions. The factor α is selected to match measured transport rates during supported drop calibration experiments. The value $\alpha = 0.9$ has generally been found to provide the best fit of the data during past work [11,12]. Mixing rules and values used for property calculations are described elsewhere [11,12].

Due to the difficulty of completely modeling internal transport processes of drops, the analysis considers two limits: (1) the infinite liquid diffusivity approximation where all properties within a drop are assumed to be uniform at each instant of time; and (2) the negligible diffusivity or "onion skin" model, where the drop surface adapts immediately to changes in local ambient conditions, while the bulk liquid remains at its initial state. These cases bound the range exhibited by real drops in sprays.

Drops leaving the injector are divided into n groups, defined by the initial position, size, velocity and direction. The subsequent motion of each group is given by

$$\vec{x}_{pi} = \vec{x}_{poi} + \int_0^t \vec{u}_{pi} dt \tag{7}$$

The instantaneous velocity is determined by integrating the equation for conservation of momentum

$$m_i \frac{d\vec{u}_{pi}}{dt} = -(\pi/8)\, d_{pi}^2\, \bar{\rho} C_D |\vec{u}_{pi} - \vec{\bar{u}}| (\vec{u}_{pi} - \vec{\bar{u}}) + \vec{a} \tag{8}$$

where the size and mass of the drop are related as follows:

$$m_i = (\pi/6)\ \rho_f d_{pi}^3 \tag{9}$$

assuming uniform liquid properties. Conservation of mass of the drop yields

$$\frac{dm_i}{dt} = -\dot{m}_i \tag{10}$$

where $\dot{m}_i$ is determined from the local concentrations at the liquid surface and in the gas [11,12].

Conservation of energy at the drop, for the infinite liquid diffusivity model, yields

$$(\rho_f C_{pf} d_{pi}/6)\ \frac{dT_{pi}}{dt} = h_i\ (\bar{T}-T_{pi}) - \dot{m}_i\ (h_{sg}-h_{sf})_i \tag{11}$$

for a simple one component liquid. In the case of the onion skin model there is no bulk heating; therefore, the energy equation becomes

$$\pi d_p^2\ h\ (\bar{T}-T_s) = \dot{m}\ (h_{sg} - h_{pf}) \tag{12}$$

where T_s is not equal to the bulk liquid temperature $T_p = T_o$ any longer. In both cases, the gas phase mass fraction of drop liquid is given by the vapor pressure relationship. The present calculations are limited to low pressures, the Clausius-Clapeyron equation suffices and the concentration of dissolved gas is negligible. The general vapor pressure relationship is

$$Y_{Fsg} = f(T_s,p) \tag{13}$$

The concentrations of other species at the drop surface, needed for property evaluations, are found from film theory analysis [7,11]

$$Y_{isg} = \bar{Y}_{i\infty}\ (1-Y_{Fsg})/(1-\bar{Y}_{F\infty}),\ i \neq F \tag{19}$$

Drop transport is modeled using film theory. This involves analysis of transport rates at Re = 0 and then multiplying the resulting expression by a correction for forced convection [7,11]. The basic expression for the drop mass transfer rate is

$$\frac{\dot{m}_{Re=0}}{2\pi d_p \rho D} = \ln\left(\frac{\bar{Y}_{F\infty}-1}{Y_{Fsg}-1}\right)$$

while the expression for the heat transfer coefficient is

$$\frac{h_{Re=0}\, d_p}{\lambda} = \left(\frac{\dot{m}\, C_p}{\pi d_p \lambda}\right) / \left[\exp\left(\frac{\dot{m}\, C_p}{2\pi d_p \lambda}\right)-1\right] \tag{16}$$

The multiplicative correction for convection was established by Faeth and Lazar [25]

$$\frac{h}{h_{Re=0}} \text{ or } \frac{\dot{m}}{\dot{m}_{Re=0}} = 1 + \frac{0.278\, Re^{1/2}\, (Pr \text{ or } Sc)^{1/3}}{(1 + 1.232/(Re\, (Pr \text{ or } Sc)^{4/3}))^{1/2}} \tag{17}$$

The standard drag coefficient for solid spheres is employed in the calculations, approximated as follows [15]:

$$\begin{aligned} C_D &= \frac{24}{Re}\left(1 + \frac{Re^{2/3}}{6}\right) \quad , \quad Re < 1000 \\ &= 0.44 \qquad\qquad , \quad Re > 1000 \end{aligned} \tag{18}$$

Gas-Phase Model. This portion of the analysis utilizes the dilute spray approximation. This implies that the void fraction is unity and that the presence of drops does not contribute directly to the generation or dissipation of turbulence (the latter effect is frequently called turbulence modulation).

The interaction between the liquid and gas phases yields an additional source term S_d on the RHS of Eq. (1). These terms are found by computing the net change of mass and momentum of each drop class i as it passes across a computational cell j.* The source terms are as follows:

Mass:
$$S_{dmj} = \sum_{i=1}^{n} \dot{n}_i (m_{i\ in} - m_{i\ out})_j \tag{19}$$

Momentum:
$$S_{d\vec{u}j} = \sum_{i=1}^{n} \dot{n}_i ((m_i \vec{u}_{pi})_{out} - (m_i \vec{u}_{pi})_{in})_j \tag{20}$$

*Only one index is needed to define a cell since the calculation is parabolic and each computational cell is defined by its radial position.

$$\text{Mixture Fraction:} \quad S_{d\bar{f}_j} = \sum_{i=1}^{n} \dot{n}_i (m_{i\ in} - m_{i\ out})_j \, Y_{of} \qquad (21)$$

where $\dot{n}_i$ is the number of drops per unit time in each class, in and out denote drop conditions entering and leaving the computational cell, and Y_{of} denotes the mass of liquid per unit mass flow rate of injected fluid. This procedure allows for full interaction between the phases, which is vital for treating the near injector region.

The gas-phase equations are solved in the same manner as the LHF model. The only change in this portion of the program involves addition of the new source terms given by Eqs. (13)-(21). The particle motion equations, Eqs. (7)-(18), are solved at the same time, in a stepwise fashion, using a second-order finite difference algorithm. The solution requires the specification of the properties of all drop classes at the injector exit.

The properties of the gas phase are computed from $\bar{f}$ and g in the same manner as the LHF model. The main change in this portion of the calculation is that the state relationships, and f, only pertain to vaporized liquid. This procedure is simplified by ignoring energy absorbed by drop heating in the infinite liquid diffusivity model. This effect could be handled by solving an additional equation for conservation of energy in the gas phase; however, the error is small at moderate pressures and the added complexity of the formulation is not merited at present.

3.4 Stochastic Separated Flow Model

The basic SF analysis provides only for deterministic trajectories for particle groups. In practical turbulent flows, however, particles are also dispersed by turbulent fluctuations. The SF model was extended to treat this effect, since the phenomena can be an important mechanism for the spread of drops in sprays. The approach used to describe particle dispersion adapts a stochastic technique proposed by Gosman and Ioannides [26].

The stochastic model involves computing the trajectories of a statistically significant sample of individual particles as they move away from the injector and encounter a random distribution of turbulent eddies--utilizing Monte Carlo methods. The general nature of the stochastic approach is illustrated in Fig. 4 for a single particle encountering three eddies. The key elements of this approach are the methods for specifying the properties of each eddy and the time of interaction of a particle with a particular eddy. The k-ε-g representation of turbulence used in the SF model provides a convenient method for prescribing these quantities.

Properties within a particular eddy are assumed to be uniform, but properties change in a random fashion from eddy to eddy. The trajectory calculation is the same as the basic SF model, involving solution of Eqs. (7)-(18); however, mean gas properties in these equations are replaced by the instantaneous properties of each eddy.

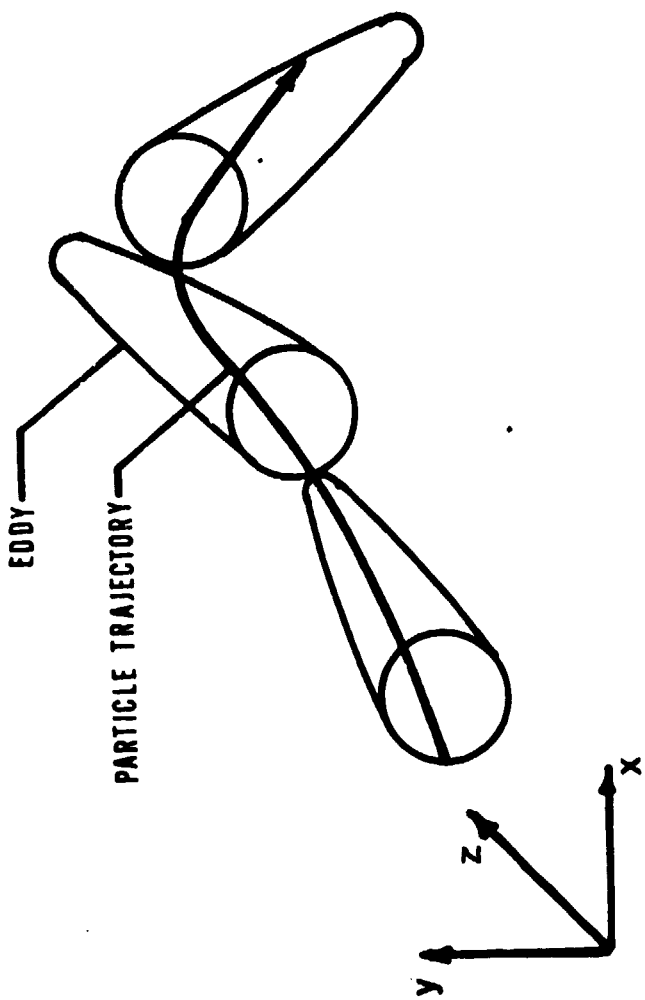

Fig. 4 Sketch of the stochastic particle trajectory model.

The properties of each eddy are found at the start of interaction by making a random selection from the pdf of velocity and mixture fraction. The velocity fluctuations are assumed to be isotropic with a Gaussian probability density distribution having a standard deviation of $(2k/3)^{1/2}$. The cumulative distribution function for the three velocity components is formed and each distribution is randomly sampled. This involves selecting three numbers in the range 0-1.0 and computing the velocity components at these three values of the cumulative distribution function.

Instantaneous physical properties for each eddy are found in a similar manner. The instantaneous mixture fraction is assumed to have clipped Gaussian probability function with mean value $\tilde{f}$ and variance g--which completely specify the pdf of mixture fraction, cf. Lockwood and Naguib [20]. The cumulative distribution function is constructed for this pdf and a single random number selection in the range 0-1.0 yields the instantaneous mixture fraction of the eddy at the sample value of the cumulative distribution function. The state relationships then provide the physical properties of the eddy, at this mixture fraction, as described earlier.

A particle is assumed to interact with an eddy for a time which is the minimum of either the eddy lifetime or the transit time required for the particle to cross the eddy. These times are estimated assuming that the characteristic size of an eddy is the dissipation length scale.

$$L_e = C_\mu^{3/4} \, k^{3/2}/\varepsilon \tag{22}$$

The eddy lifetime is computed from the following:*

$$t_e = L_e/(2k/3)^{1/2} \tag{23}$$

The transit time of a particle is found from the linearized equation of particle motion in a uniform flow

$$t_t = -\tau \ln \left(1 - L_e/(\tau|\vec{u}'' - \vec{u}_p''|)\right) \tag{24}$$

where $\vec{u}'' - \vec{u}_p''$ is the velocity difference at the start of the interaction and τ is the linearized particle relaxation time

$$\tau = 4\rho_p \, d_p/(3\rho C_D|\vec{u}'' - \vec{u}_p''|) \tag{25}$$

When $L_e > \tau|u'' - \bar{u}_p''|$, the linearized stopping distance of the particle is smaller than the characteristic length scale of the eddy and Eq. (24) has no solution. In this case, the eddy has captured the particle and the interaction time is the eddy lifetime.

---

*These prescriptions are slightly different than those of Gosman and Ioannides [26], but have been successfully calibrated [15].

The remainder of the computation proceeds similar to the deterministic case. The only change is that the source terms of Eqs. (19)-(21) are computed for the random walk trajectories of the particles--as opposed to their deterministic solution. The main disadvantage of the stochastic method is that more particle trajectories must be considered in order to obtain statistically significant particle properties.

The stochastic model yields estimates of both mean and fluctuating particle properties at each point in the flow. This information is useful, since these properties can be measured and provide a good test of model performance. A notable feature of the model is that added empiricism is minimal.**

4. Results and Discussion

The apparatus was assembled during this report period and measurements have begun. The model was evaluated using existing results for particle-laden flows during the report period.

In the following, results for particle-laden flows will be considered first, followed by the initial findings for nonevaporating sprays.

4.1 Particle-Laden Flows

A search of the literature revealed a substantial data base of measurements in particle-laden jets. Table 3 is a summary of the results employed to evaluate the models. The theoretical findings of Hinze [27], concerning the dispersion of infinitely small particles from a point source in an isotropic turbulent flow were employed to calibrate the stochastic model, similar to Gosman and Ioannides [26]. The remaining measurements were employed for model evaluation. This included measurements of single-particle dispersion in a turbulent duct flow by Snyder and Lumley [28]; and in particle-laden jets by McComb and Salih [30], Laats and Frishman [31], and Levy and Lockwood [32].

The calibration results are illustrated in Fig. 5. Stochastic model predictions from Gosman and Ioannides [26] and the present model are shown, along with the exact analytical results from Hinze [27]. The present model is in good agreement with the exact results, indicating satisfactory calibration. Gosman and Ioannides [26] model, as posed, yields poorer agreement due to a computational error in their original work that has since been corrected [33].

Predictions of the present stochastic SF model, as well as the version of Gosman and Ioannides [26] and the measurements of Snyder and Lumley [28] are illustrated in Fig. 6. These experiments involved dispersion of individual particles which were isokinetically injected into a uniform turbulent flow downstream of a grid. The two models yield nearly the

---

*In fact, no new constants must be formally prescribed; however, Eqs. (22) and (23) implicitly involve constants of proportionality although their values turned out to be unity when the model was calibrated.

Table 3. Summary of Measurements in Particle-Laden Flows[a]

Source	Configuration	Loading Ratio	Reynolds Number	Particle Type	Particle Size (μm)	Particle Density (kg/m^3)
Hinze [27]	One-dimensional flow, isotropic turbulence	Single particles	--	Theoretical	0	0
Snyder and Lumley [28]	Duct flow, grid-generated turbulence	Single particles	--	hollow glass	46.5	260
				corn pollen	87	1,000
				glass	87	2,500
				copper	46.5	8,900
Yuu et al. [29]	Jet	0.0008-0.004	11,000- 56,000	fly ash	20	2,000
McComb and Salih [30]	Jet	Small	5,000- 15,000	titaniumdioxide	2.3	4,260
				tungsten	5.7	19,300
Laats and Frishman [31]	Jet	0.3-1.4	66,000-137,000	sand	17-80	
Levy and Lockwood [32]	Jet	1.14-3.50	20,000	sand	215-1060	2,250

[a]Continuous phase was air.

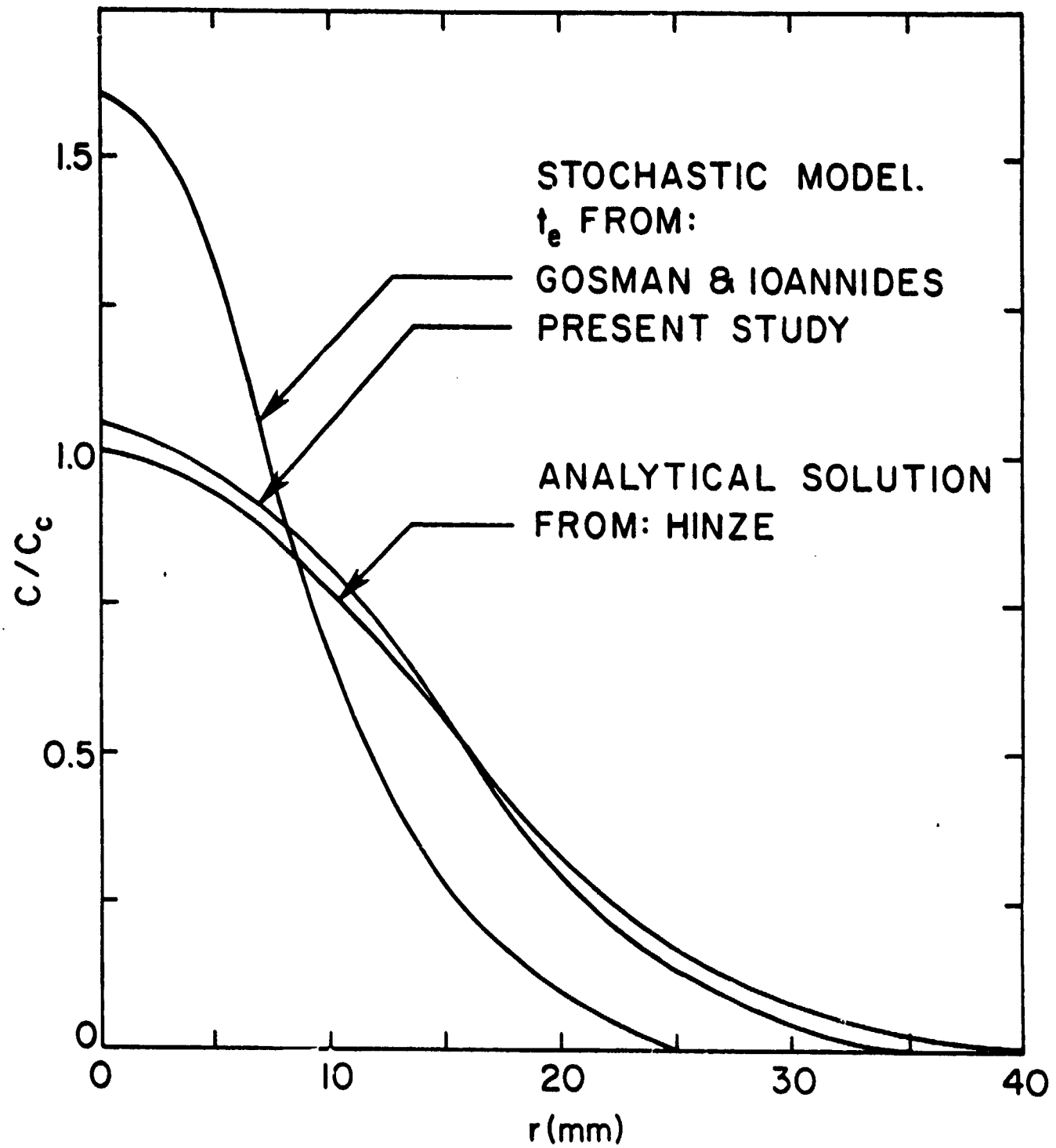

Fig. 5 Analytical and stochastic solutions for the dispersion of small particles in homogeneous isotropic turbulent flow with long diffusion times.

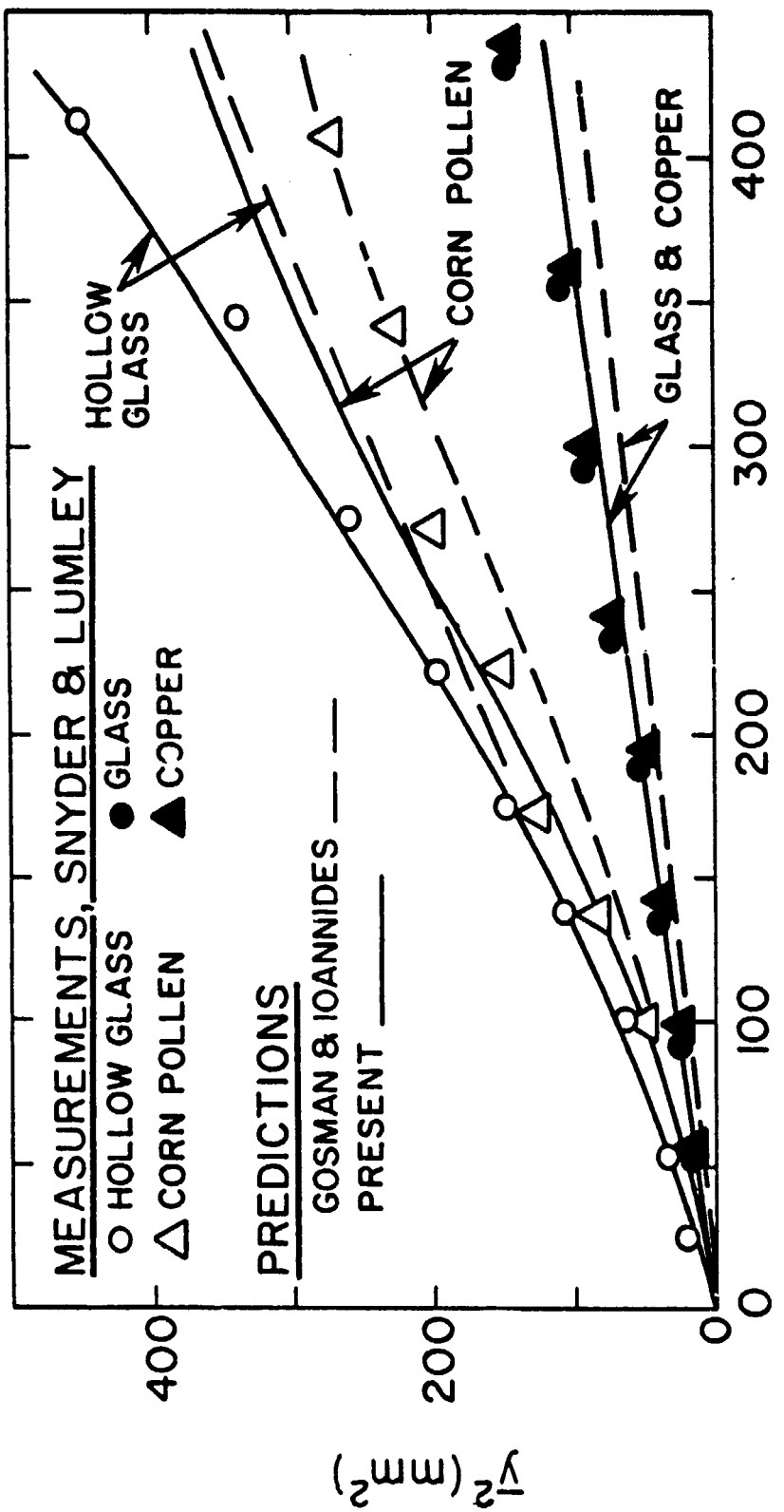

Fig. 6. Predicted and measured particle dispersion in a uniform, grid-generated turbulent flow.

same results for heavy particles where the calibration error of [26] has little effect. The present model yields better agreement for the lighter particles where calibration of characteristic eddy time and length scales is more significant since light particles tend to be captured by the eddies.

Significance of particle dispersion in particle-laden jets can be better appreciated from the results appearing in Fig. 7. The particle concentration measurements of Yuu et al. [29] are illustrated along with three predictions: (1) the LHF model, (2) the SF model with no consideration of turbulent dispersion, and (3) the stochastic SF model. Predictions in each case are given at values of x/d which limit the data range. The LHF model overestimates the rate of particle spread, since it neglects slip between the phases. On the other hand, the deterministic SF model underestimates the rate of spread, since radial particle velocities are only generated by the $\bar{v}$ velocity component--which is relatively small (this version also indicates that the particles are confined to a progressively narrower range of r/x as x/d increases, which is also not observed). In contrast, the stochastic SF model yields good agreement with the measurements.

Predictions of the LHF and stochastic SF models are compared with data from Yuu et al. [29] at various operating conditions in Fig. 8. The stochastic SF model yields good predictions while the LHF model continues to overestimate the rate of particle spread.

The measurements of McComb and Salih [30] are compared with the model in Figs. 9 and 10. The results are generally similar to those obtained with the Yuu et al. [29] measurements. An interesting feature of these measurements is that the particle spread rate begins to approach the LHF predictions as x/d becomes large, since the large eddies in this region tend to capture the particles more effectively.

Predictions and measurements for the test conditions of Laats and Frishman [31] are illustrated in Figs. 11 and 12. These authors considered much higher mass loadings of particles (mass of particles/mass of gas) than Refs. 27-30. The agreement between the stochastic SF predictions and measurements is comparable to that observed for the Yuu et al. [29] and McComb and Salih [30] data, except at the highest particle mass loading where the stochastic model overestimates the rate of spread of the particles. This suggests that turbulence levels are lower under these conditions than predicted, which could result from the extraction of turbulence energy by the drag of the particles. This phenomena, which is called turbulence modulation [34], is not considered in the present models.

Additional evidence of effects of particles on turbulence properties is provided by the results of Levy and Lockwood [32] illustrated in Fig. 13. Mean gas velocities are predicted reasonably well; however, longitudinal fluctuations of gas velocity are generally underestimated for large particles at high loading ratios. In this case, the high rate of slip of the particle through the gas enhances turbulent fluctuations in a manner that is not considered in the model.

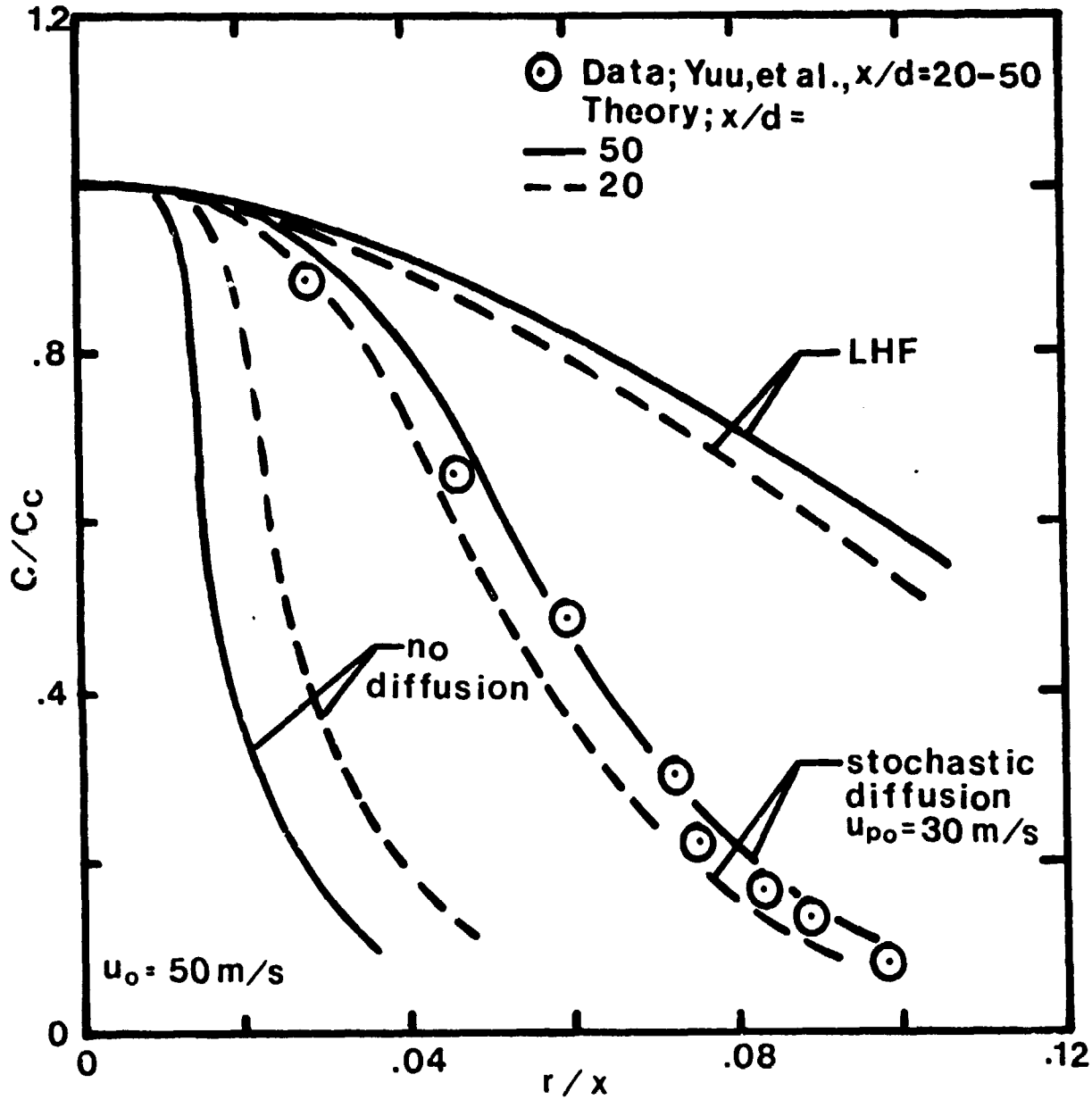

Fig. 7 Turbulent particle dispersion in an axisymmetric jet Data of Yuu et al. [29].

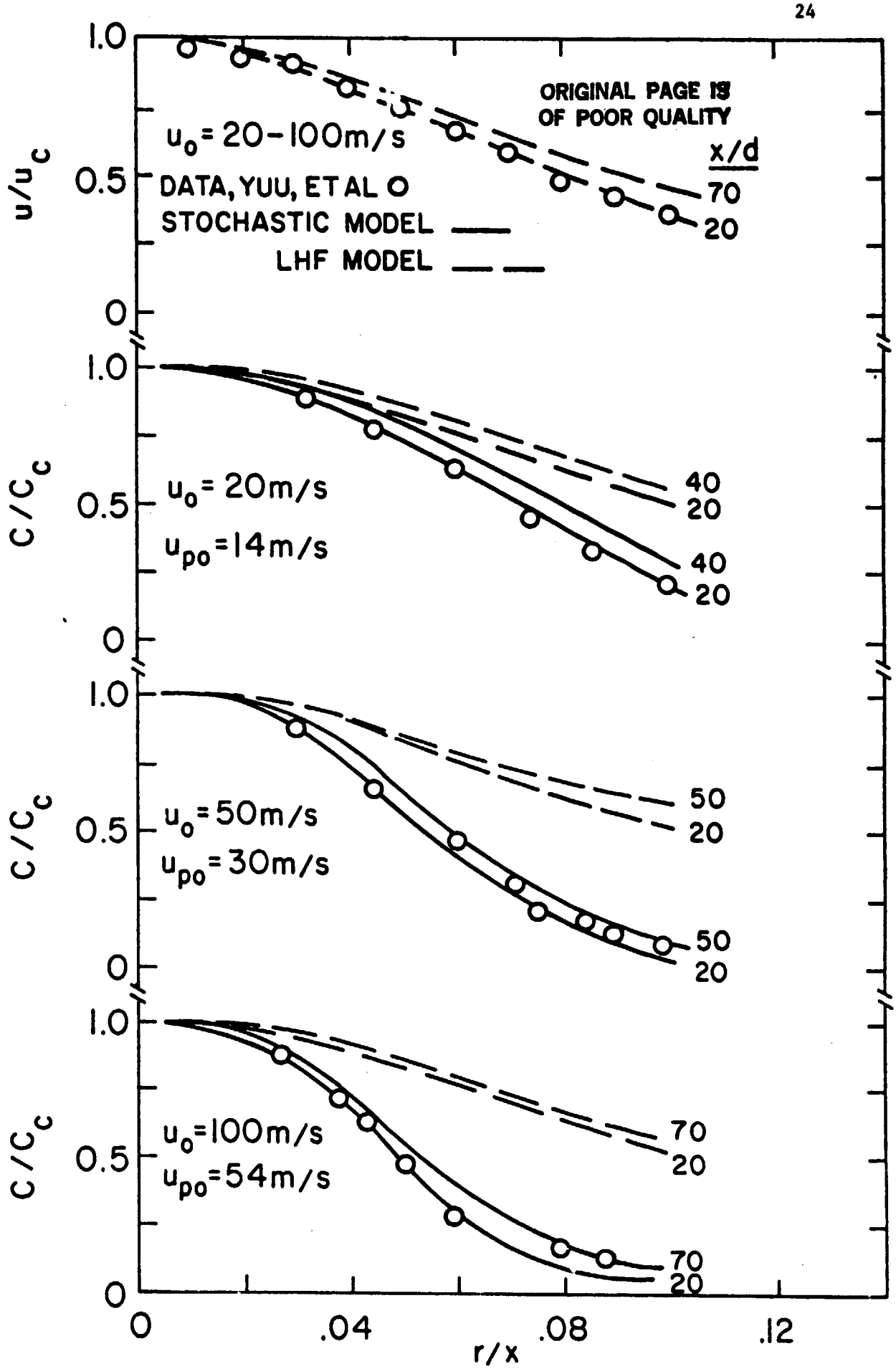

Fig. 8. Predicted and measured axial gas velocities and particle concentrations in a dust-laden air jet with particle diameter of 20 μm. Data of Yuu et al. [29].

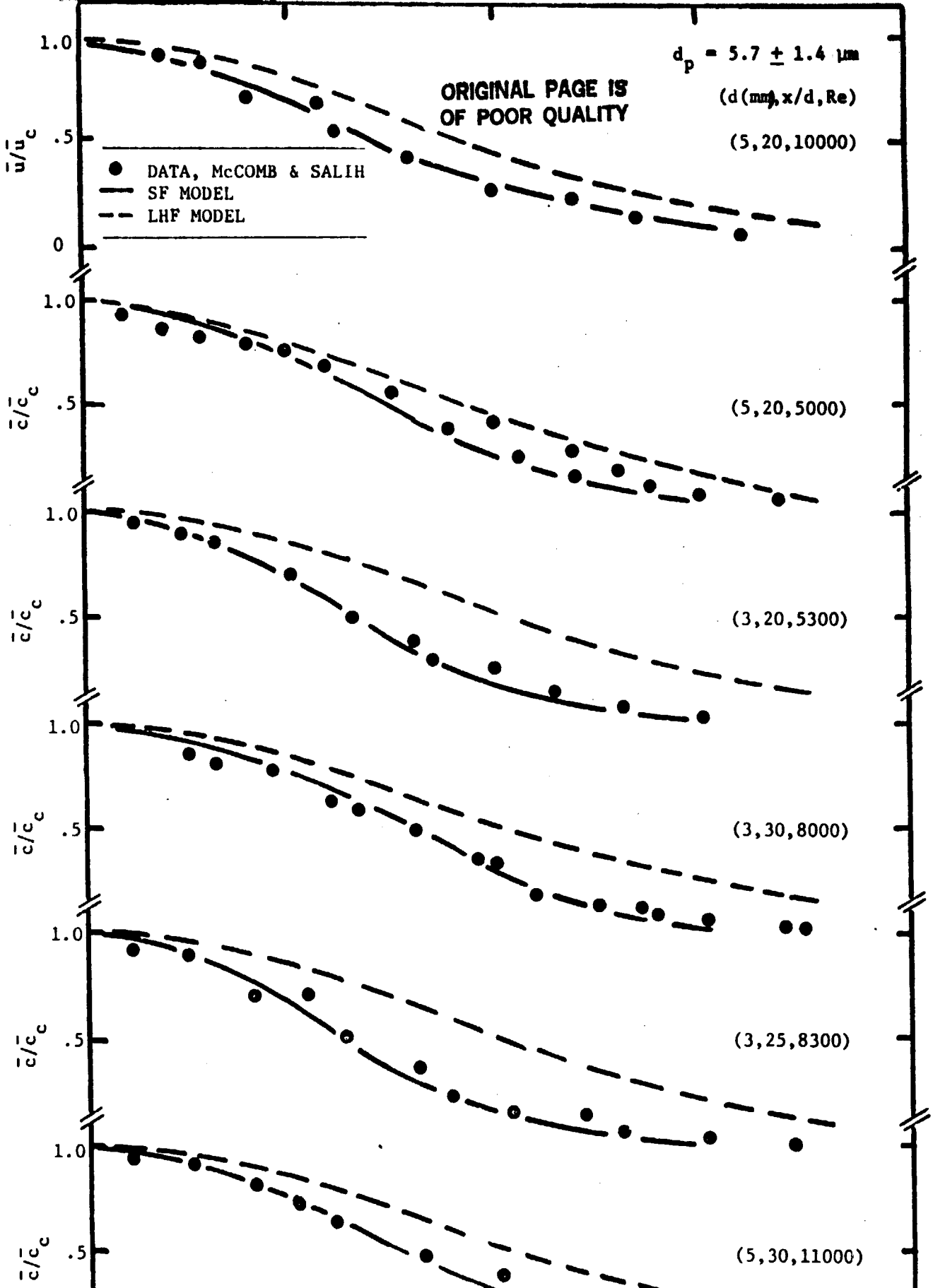

Fig. 9 Predicted and measured particle concentrations in particle-laden jets. Data of McComb and Salih [30].

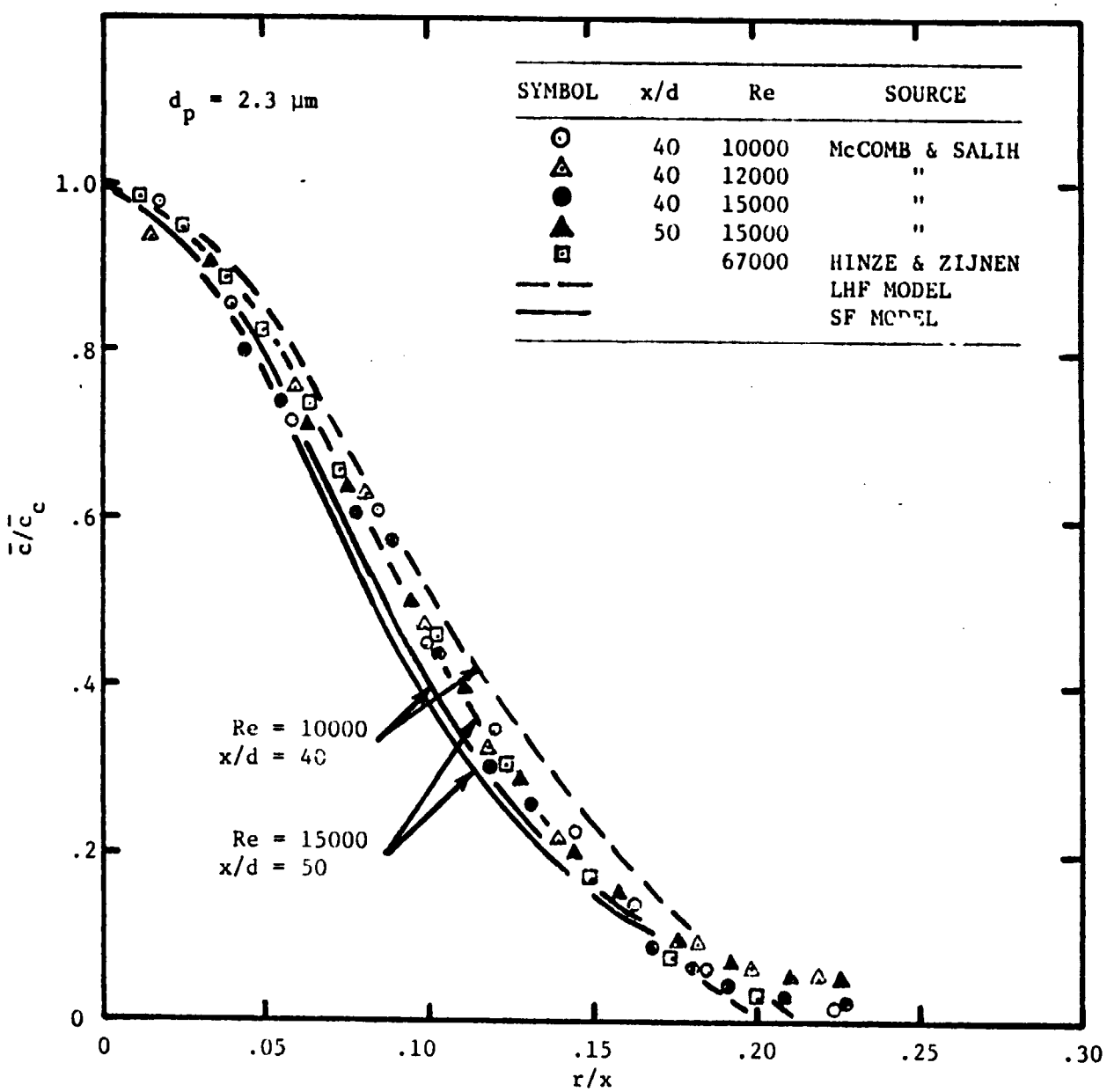

Fig. 10 Predicted and measured axial velocities and particle concentrations in particle-laden jets. Data of McComb and Salih [30].

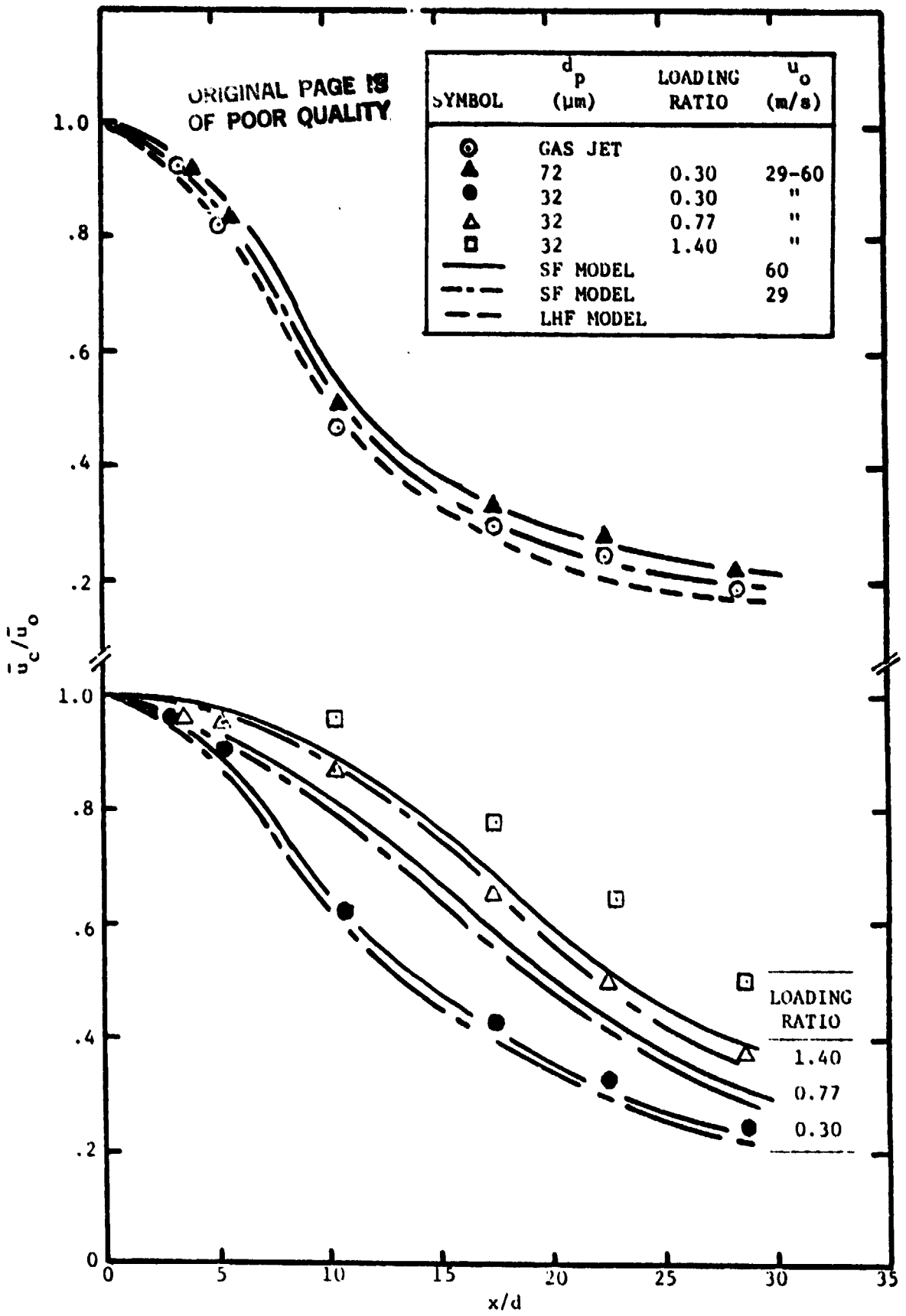

Fig. 11 Predicted and measured axial mean velocities along the centerline of particle-laden jets. Data of Laats and Frishman [31].

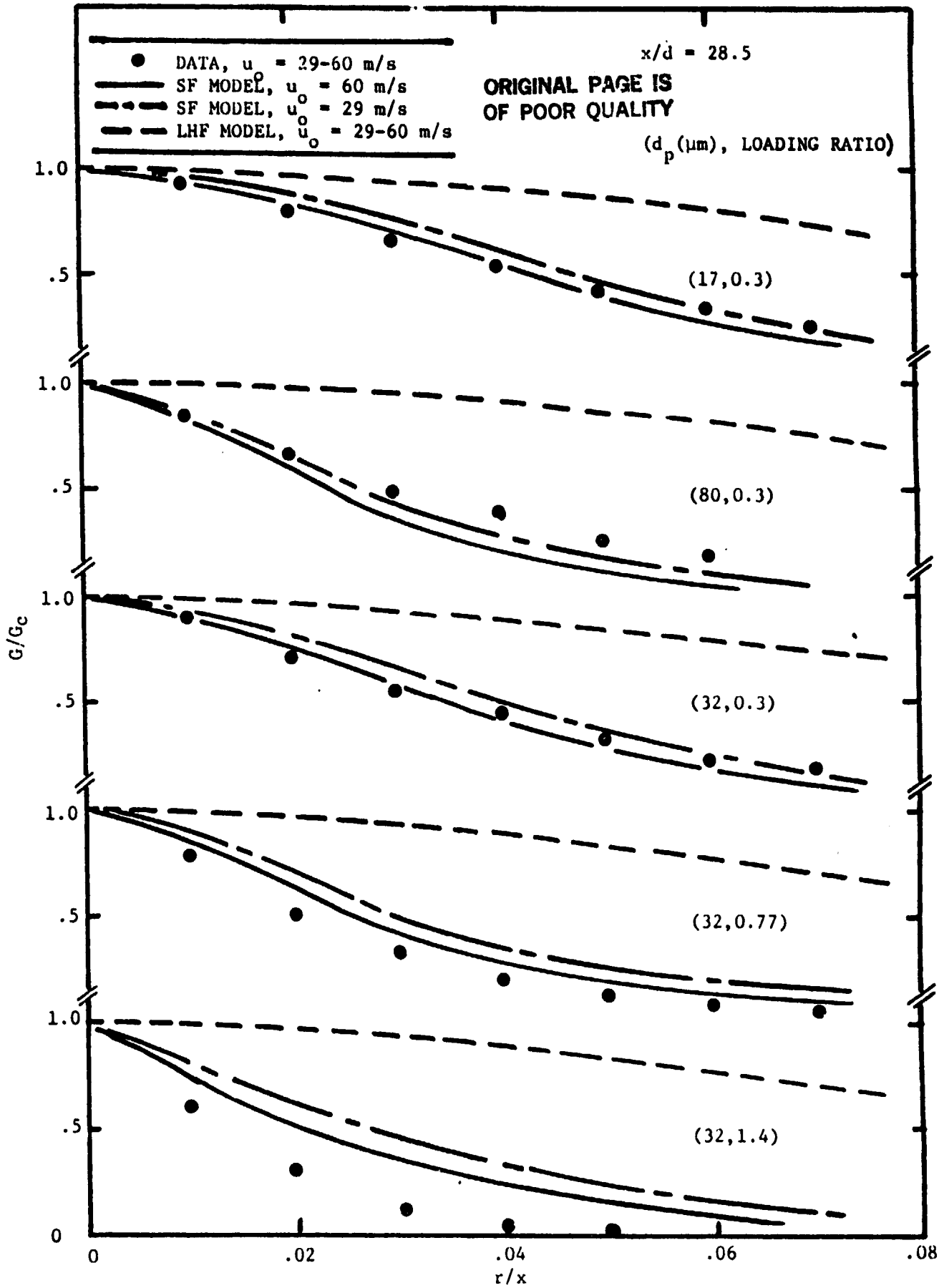

Fig. 12 Predicted and measured particle mass velocities in particle-laden jets. Data of Laats and Frishman [31].

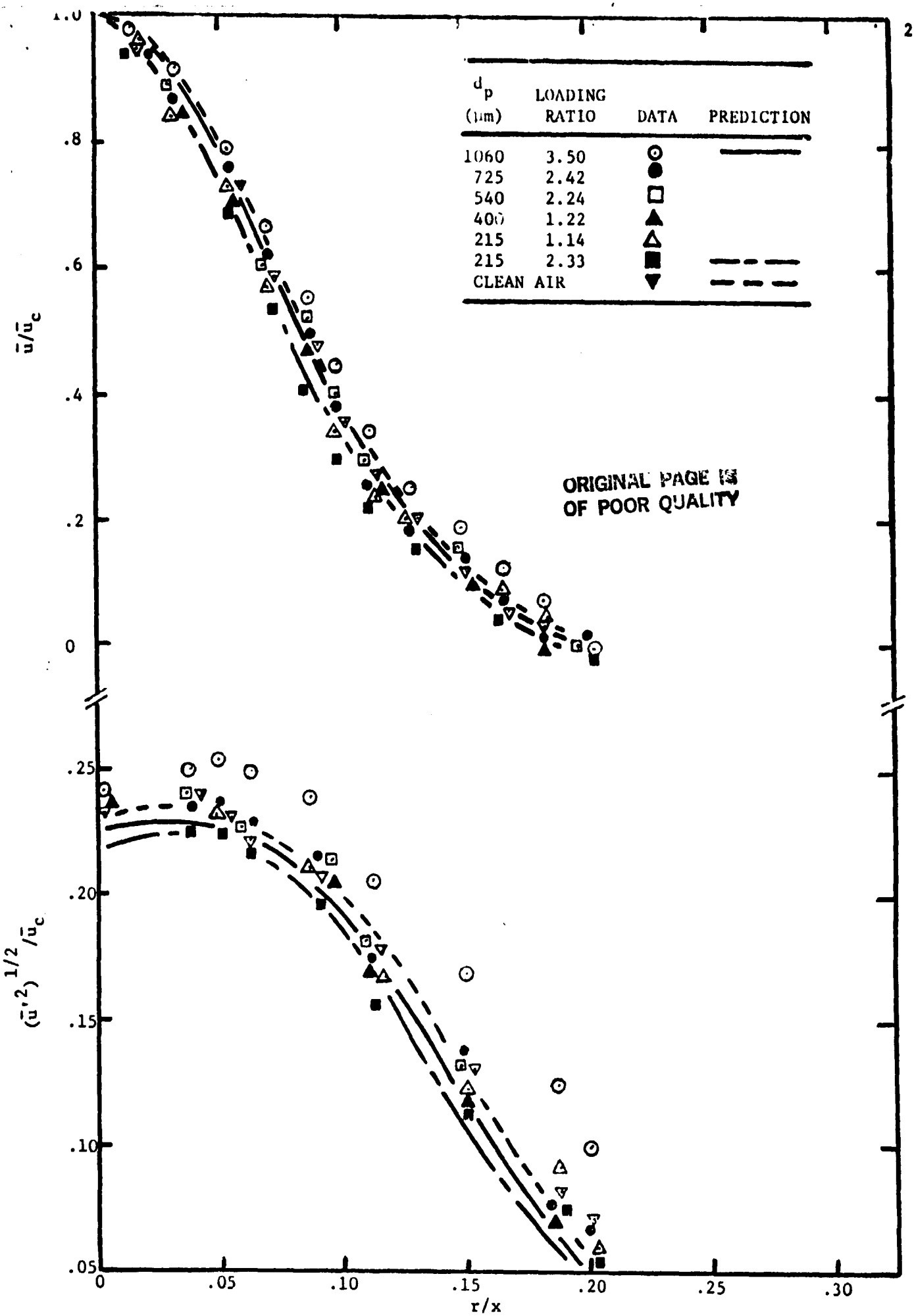

Fig. 13 Predicted and measured mean and fluctuating gas velocities in particle-laden jets. Data of Levy and Lockwood [32].

Figure 14 is an illustration of mean and fluctuating particle velocities for the data of Levy and Lockwood [32]. Predictions of mean particle velocity agree reasonably well with measurements at all conditions. Predicted particle fluctuating velocities, however, underestimate the measurements for all but the smallest particles in this data base. This effect can only be attributed to operation of the particle-gas mixing system (a worm gear drive followed by a straight but relatively short length of ducting) since the large particles have a relatively moderate change in velocity over the flow field. Unfortunately, Levy and Lockwood [32] did not make measurements of initial conditions at the duct exit to help clarify this effect.

Our analysis of existing data for particle-laden jet was inhibited by lack of information concerning initial conditions in all cases. The original authors generally felt that there was negligible slip between the phases at the injector exit; however, analysis of the injector passage flow invariably showed that this was not the case. Thus, we conclude that the results of the model are encouraging; however, more information on initial conditions is needed for decisive evaluation. Furthermore, the model may require extension to include effects of turbulence modulation before adequate predictions can be obtained in dense particle flows and sprays.

4.2 Nonevaporating Sprays

The apparatus described in Section 2 was designed, fabricated and assembled. Testing thus far has been devoted to the isothermal air jet and noncombusting sprays.

The main objective of the air jet experiments is to check the operation of the apparatus and to establish LDA procedures for measuring mean and fluctuating gas velocities. The new results are being compared with existing measurements of Shearer et al. [21], Mao et al. [22], Wygnanski and Fiedler [36], and Hetsroni and Sokolov [37]. The measurements involve axial profiles of mean velocity and streamwise velocity fluctuations as well as radial profiles of these quantities and Reynolds stress. These measurements are being conducted for a subsonic air jet passing from the injector, with jet Reynolds numbers greater than 10^4, to ensure reasonably well-developed turbulent flow. Jet exit conditions are defined by measuring the air mass flow rate and the thrust on the injector.

The measurements are being conducted with the single-channel LDA, using various beam orientations to obtain the velocity components and the Reynolds stress--similar to earlier work [21-22]. Results obtained to date indicate that adequate seeding levels have been achieved, flow disturbances are negligible, the jet is properly aligned, and the results of the measurements are in good agreement with past work.

Testing has begun to examine the properties of nonevaporating sprays. Thus far, two conditions have been established for detailed structure measurements: (1) a spray with a SMD of 30 microns which represents a near LHF condition, and (2) as spray with a SMD of 70 microns which requires SF modeling for reasonable accuracy. Thus far initial conditions have been measured--SMD, mass flow rates and injector thrust. Detailed structure measurements are now in progress using the LDA for gas velocities.

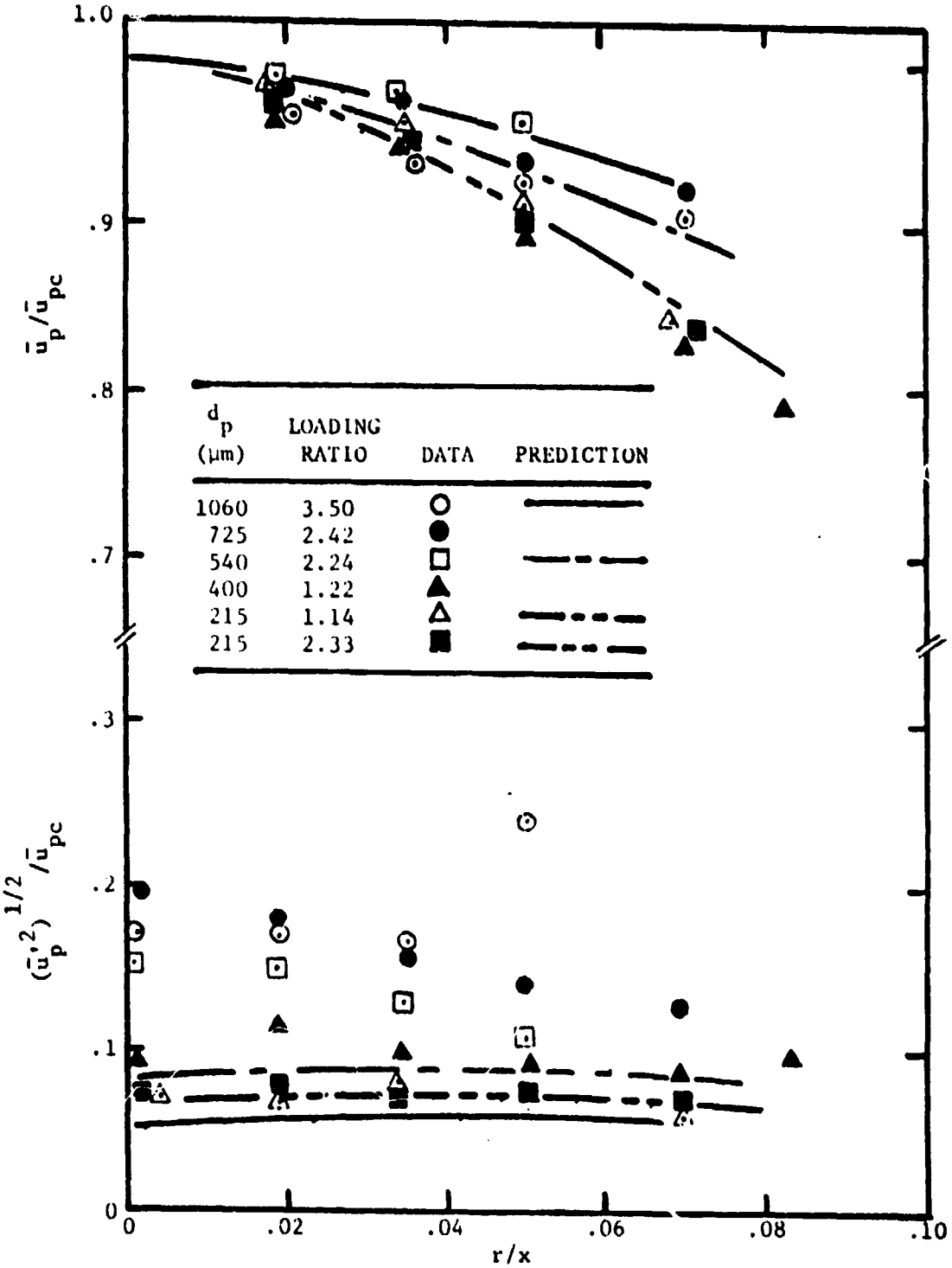

Fig. 14 Predicted and measured mean and fluctuating particle velocities in particle-laden jets. Data of Levy and Lockwood [32].

Modeling efforts are now being directed to nonevaporating sprays. LHF model calculations have been completed for present test conditions. SF model calculations will be undertaken as soon as initial conditions for the experiments have been fully defined. In addition to these measurements, recent results reported by Yule et al. [35] are also being considered. These results with nonevaporating sprays will help indicate whether modeling of steady spray processes will require consideration of particle collisions and shattering.

5. Status and Plans for the Next Report Period

The spray apparatus has been constructed and measurements are currently in progress for nonevaporating sprays. Based on progress to date, all testing on noncombusting sprays should be complete at the end of the current grant period. The extent to which the LDA visibility method for measuring drop-size and velocity distributions can be applied to these results will depend on prompt delivery of equipment and problems encountered in making the system operational. The results of the investigation are not contingent on the use of this technique, however, since the availability of the equipment was not known at the time the study was planned.

The LHF and SF models have been developed and coded for use on the computer. Turbulence model constants used for these calculations were established during earlier work [21-22]. Computations for solid particle flows have generally established the usefulness of the stochastic particle dispersion model for dilute flows, although some uncertainty remains due to inadequate specification of initial conditions throughout the existing data base. Results to date suggest that there may be significant effects of turbulence modulation in dense particle flows, however, additional information on flow structure is needed to rationally complete this extension. Comparisons between predictions and both existing [35] and the present new measurements will be undertaken during the next report period. These results will help determine whether model extensions are needed in order to treat drop collisions and shattering, as well as effects of turbulence modulation.

REFERENCES

1. Anderson, O. L., Chiappetta, L. M., Edwards, D. E. and McVey, J. B., "Analytical Modeling of Operating Characteristics of Premixing-Preevaporating Fuel-Air Mixing Passages," Report No. UTRC 80-102, Vol. I and II, United Technologies Research Center, East Hartford, 1980.

2. Bruce, T. W., Mongia, H. C. and Reynolds, R. S., "Combustor Design Criteria Validation," Vol. I-III, USARTL-TR-78-55(A,B,C), Fort Eustis, VA, 1979.

3. Mongia, H. C. and Smith, K., "An Empirical/Analytical Design Methodology for Gas Turbine Combustors," AIAA Paper No. 78-998 (1978).

4. Butler, T. D., Cloutman, L. D., Dukowicz, J. K., Ramshaw, J. D. and Krieger, R. B., Combustion Modeling in Reciprocating Engines (J. N. Mattavi and C. A. Amann, ed.), pp. 231-264, Plenum Press, New York, 1980.

5. Alpert, R. L. and Mathews, M. K., "Calculation of Large-Scale Flow Fields Induced by Droplet Sprays," Technical Report No. FMRC J.1.OEOJ4.BU, Factory Mutual Research Corporation, Norwood, MA, 1979.

6. Faeth, G. M., Prog. Energy Combust. Sci. 3, 191 (1977).

7. Mellor, A. M., Seventeenth Symposium (International) on Combustion, pp. 377-387, The Combustion Institute, Pittsburgh, 1979.

8. Williams, A., Combustion of Sprays of Liquid Fuels, Elek Science, London, 1976.

9. Williams, A., Prog. Energy Combust. Sci. 2, 167 (1976).

10. Faeth, G. M., "Spray Combustion Models--A Review," AIAA Paper No. 79-0293, 1979.

11. Faeth, G. M., "Evaporation and Combustion of Sprays," to be published, 1982.

12. Shearer, A. J., Tamura, H. and Faeth, G. M., J. of Energy 3, 271 (1979).

13. Mao, C-P., Szekely, G. A., Jr. and Faeth, G. M., J. of Energy 4, 78 (1980).

14. Mao, C-P., Wakamatsu, Y. and Faeth, G. M., Eighteenth Symposium (International) on Combustion, pp. 337-347, The Combustion Institute, Pittsburgh, 1981.

15. Shuen, J-S., Chen, L-D. and Faeth, G. M., Evaluation of a Stochastic Model of Particle Dispersion in a Turbulent Round Jet," AIChE J., in press.

16. Solomon, A. S. P., Rupprecht, S. D., Chen, L-D. and Faeth, G. M., "Atomization and Combustion Properties of Flashing Injectors," AIAA Paper No. 82-0300, 1982.

17. Jones, A. R., Prog. Energy Combust. Sci. 3, 230 (1977).

18. Bachalo, W. D., Hess, C. F. and Hartwell, C. A., "An Instrument for Spray Droplet Size and Velocity Measurements," ASME Paper No. 78-WA/GT-13, 1979.

19. Gosman, A. D., Lockwood, F. C. and Syed, S. A., Sixteenth Symposium (International) on Combustion, pp. 1543-1555, The Combustion Institute, Pittsburgh, 1977

20. Lockwood, F. C. and Naguib, A. S., Combust. Flame 24, 109 (1975).

21. Shearer, A. J. and Faeth, G. M., "Evaluation of a Locally Homogeneous Model of Spray Evaporation," NASA CR-3198, 1979.

22. Mao, C-P., Szekely, G. A., Jr. and Faeth, G. M., "Evaluation of a Locally Homogeneous Flow Model of Spray Combustion," NASA CR-3202, 1980.

23. Gordon, S. and McBride, B. J., "Computer Program for Calculation of Complex Chemical Equilibrium Compositions, Rocket Performance, Incident and Reflected Shocks, and Chapman-Jouguet Detonations, NASA SP-273, Washington, 1971.

24. Spalding, D. B., GENMIX: A General Computer Program for Two-Dimensional Series, Parabolic Phenomena, Pergamon Press, Oxford, 1978.

25. Faeth, G. M. and Lazar, R. S., AIAA J. 9, 2165 (1971).

26. Gosman, A. D. and Ioannides, E., "Aspects of Computer Simulation of Liquid-Fueled Combustors," AIAA Paper No. 81-0323, 1981.

27. Hinze, J. O., Turbulence, 2nd Ed., McGraw-Hill, New York, 1975.

28. Snyder, W. H. and Lumley, J. L., J. Fluid Mech. 48, 41 (1971).

29. Yuu, S. Yasukouchi, N., Hirosawa, Y. and Jotaki, T., AIChE J. 24, 509 (1978).

30. McComb, W. D. and Salih, S. M., J. Aerosol Sci. 8, 171 (1977); also Ibid., 9, 299 (1978).

31. Laats, M. K. and Frishman, F. A., Fluid Dynamics 5, 333 (1970); also Heat Transfer-Soviet Res. 2, 7 (1970).

32. Levy, Y. and Lockwood, F. C., Combust. Flame 40, 333 (1981).

33. Gosman, A. D., Personal Communication, 1981.

34. Al Taweel, A. M. and Landau, J., Int. J. Multiphase Flow 3, 341 (1977).

35. Yule, A. J., Ah Seng, C., Felton, P. G., Ungut, A., Chigier, N. A., Combustion and Flame 44, 71 (1982).

36. Wygnanski, I. and Fiedler, H. E., J. Fluid Mech. 38, 577 (1969).

37. Hetsroni, G. and Sokolov, M., J. App. Mech. 38, 314 (1971).